16TH EUROPEAN CONFERENCE ON EARTHQUAKE ENGINEERING
THESSALONIKI 18 - 21 JUNE 2018

DEVELOPMENTS IN ROCKING WALL-FRAME SYSTEMS

Mark GRIGORIAN[1], Mozhgan KAMIZI[2], Shayan TAVOUSI[3], Hadiseh MOHAMMADI[4]

ABSTRACT

The behavior of Rocking Wall Moment frame (RWMFs) can best be visualized by the Moment-Frame (MF) holding the wall in place, and the Rigid Rocking Wall (RRW) providing damping and imposing uniform drift along the height of the frame. The proposed concepts lead to an efficient structural configuration with provisions for Self-centering (SC), reparability, performance control, damage tolerance and Collapse Prevention (CP). Exact, unique, closed form formulae have been provided to assess the CP and SC capabilities of the system. The purpose is to provide an informative account of RWMF behavior for preliminary design and educational purposes. Parametric examples have been provided to verify the validity of the proposed solutions.

Keywords: Rocking wall-frames; Uniform drift; Collapse prevention; Re-centering; Reparability

1. INTRODUCTION

The use of rocking systems with gap opening walls and beams, have been studied extensively in recent years. The important conclusion drawn from current experience is that rocking can provide improved seismic performance with CP and RC. The current paper focuses on the performance of the RWMFs rather than isolated rocking cores and reflects parts of a research program currently being conducted by the authors and their colleagues, (Grigorian 2017a and b). The utility of any rocking systems, as part of a building structure, depends upon the following conditions;

1-*The relative stiffnesses of the structure and the rocking system;*
2- *Local seismicity and structural archetype.*
3- *Interactions of the two systems at common interfaces.*
4- *The response of the freestanding MF on its own.*

These conditions have been employed to propose a new building architype that incorporates Post-tensioned (PT) RRWs, Link Beams (LBs), Buckling Restrained Braces (BRBs) and a Grade Beam Restrained Moment Frame (GBRMF). The most compelling utility of the proposed solution is that it allows RWMFs to be designed as damage tolerant systems and/or as CP structures. The analytical model of the proposed system is presented in Fig. 1(a). The fundamental idea behind the proposed methodology

[1] Senior Structural Engineer, MGA Structural. Eng. Inc., 111 N. Jackson St. Glendale, CA 91206, US, markarjan@aol.com [2] Graduate student, Department of Civil Engineering, Faculty of Engineering, Golestan University , Gorgan, Iran,
mkamizi11 @gmail.com
[3] Graduate student of Earthquake Engineering, International Institute of Earthquake Engineering and Seismology, Tehran, Iran, shayantavousi@gmail.com
[4] Graduate student of Earthquake Engineering, International Institute of Earthquake Engineering and Seismology, Tehran, Iran, H.mohammadi@iiees.ac.ir

is that seismic structural response is mainly a function of design and detailing rather than analysis. The lateral load profile is asserted rather than expected. Both, strength and stiffness are induced rather than investigated. Instability and failure modes are enforced rather than tested. CP and SC features are integrated as parts of the drift reduction capabilities. The more significant findings incorporated as basic assumptions or direct analytic input can be summarized as follows;

- RRWs act as vertical simply supported beams rather than a fixed base cantilevers.
- Axial stiffnesses of the BRBs, LBs and the RRW can be replaced by equivalent rotational stiffnesses.
- RRWs suppress higher modes of vibration to lower than those associated with axial deformations.
- RRWs may be considered rigid if their maximum drift does not exceed 10 % of the allowable drift.
- RWMF remain Single Degree of Freedom systems throughout the loading history of the structure.
- Drift concentration is either nil or insignificant during all loading stages of the structure.

2. DESIGN LED SYSTEM DEVELOPMENT

In design led development the structure is configured to perform as expected rather than tested for compliance with the same requirements. The first step in developing the proposed system is to identify the flaws and weaknesses associated with conventional, fixed base, dual systems and to offer rational alternatives. However, adapting the following design strategies can alleviate most or all such flaws:

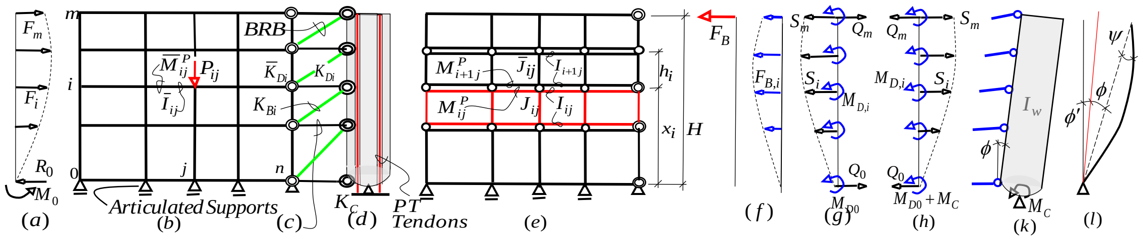

Figure1. (b) GBRMF, (c) LBs, (d) RRW, (e) Equivalent sub-frames, (f) BRB shear distribution, (g) LB forces acting on MF (h) LB forces acting on RRW, (k) RRC base moment, (l) RRW displacements

- Increasing energy dissipation, through steel tendon stretching or similar devices
- Providing structural dampers and devices, such as LBs, BRBs, friction devices, etc.
- Reducing the global stiffness in order to increase natural periods of vibrations.
- Making demand capacity ratios of as many members as close to unity as possible.
- By allowing the first mode of vibrations to suppress all higher modes.
- Enforcing sway type collapse mechanism to prevent soft story failure.
- Reducing drift concentration, thereby improving structural performance.
- Reducing damage by using specific boundary support conditions such as those in GBRMFs.
- Increasing repairability, by limiting damage to beams and replaceable items only.

These conditions have been implemented as essential attributes of the RWMF, Figs. 1(b), (c) and (d). In this scheme i and j are the joint coordinates of a $m \times n$ MF. $\bar{I}_{i,j} = I_{i,j} + I_{i+1,j}$ and $\bar{J}_{ij} = J_{ij}$, and $\bar{M}^P_{i,j} = M^P_{i,i} + M^P_{i+1,j}$ and $\bar{N}^P_{i,j} = N^P_{i,j}$ stand for moments of inertias and plastic moments of resistance of beams and columns related to joint ij respectively. The rotational stiffness of the RRW, Fig. 1(d), is symbolized as K_C. The equivalent rotational stiffnesses of the tendon systems connecting the LBs to the RRW and the MF are given as $K_{D,i}$ and $\bar{K}_{D,i}$ respectively. $K_{B,i}$ is the equivalent rotational stiffness of the BRB at level i. In this paper supplementary devices have been used as means of CP and SC rather than damping. The advantages of the proposed improvements may be summarized as follows;

- The new system is ideally suited for reducing drift and preventing soft story failure.
- The new system lends itself well to SC, CP and damage reduction.
- The proposed system attracts less residual stresses and deformations due seismic effects.
- No major anchor bolt, base plate and footing damage can occur due to seismic moments.

- Gap openings dissipate energy and provide opportunities for SC and CP.
- RRWs can be used as elements of structural control for pre and post-earthquake conditions.
- The drift profile is not sensitive to minor changes in wall stiffness.
- RWMFs have longer natural periods of vibration and attract smaller seismic forces.
- The displacement profile remains a function of the same single variable for all loading conditions.
- The structure is a SDOF system, and as such lends itself well to equivalent energy studies.
- The limit state drift ratios are smaller than those of frames with fixed boundary support conditions
- The magnitude and distribution of *P*-delta moments are more favorable than in similar MFs.
- The restraining effects of BRBs can be expressed as notional equivalent overturning moments;

The proposed system consists of five essential components; In GBRMFs plastic hinges are forced to form at the ends of the grade beams. LBs, fully bearing gap-opening devices tend to expand the frame beyond its original span length, Garlock, et al. (2007), Dowden (2011). Span expansion induces drift

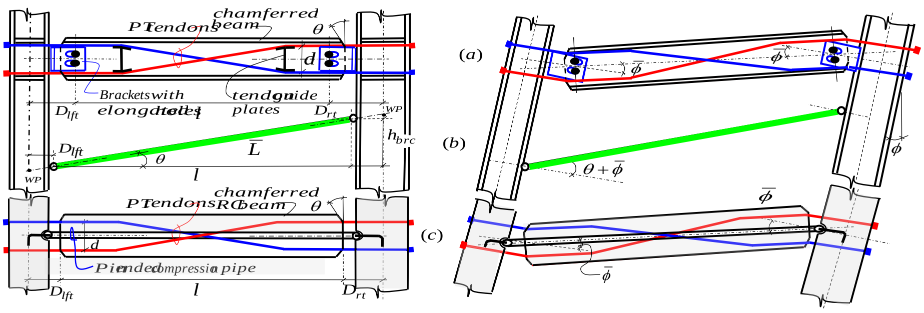

Figure 2. (a) Chamfered steel LB, (b) BRB (c) Chamfered reinforced concrete LB.

concentration, additional column moments and damages the diaphragms. These effects can be avoided by truncating the ends of the LBs, Figs. 2(a) and 2(c). The proposed LBs consist of pin ended beams that contain prearranged tendons. In order to avoid contact between the column and the truncated ends, the width of the initial gap should be larger than $\bar{\phi} d / 2$.

- The layout, cross sectional areas, guide plates, the PT forces etc., should be assessed in terms of the required drift angle, SC and CP requirements. The cable layouts presented in Fig. 2 have been devised to reduce loss of stretching due to simultaneous gap opening and closing at both ends of the LB.

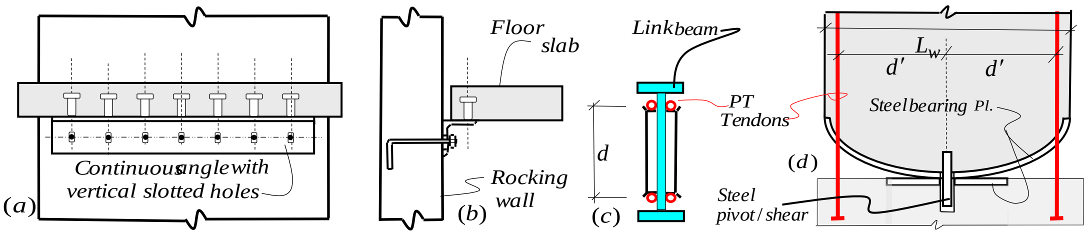

Figure 3. (a) and (b) Wall-slab shear connection, (c) LB section, (d) Rocking wall base and cables

- Seismic shear is transferred to the RWMF through direct shear, PT tendons, LBs, BRBs, as well as shear connectors between the slab and the RRW, Figs. 3 (a) and (b). The physical separation between the slab the wall and the LBs prevents the slab and the wall from being damaged. Detail 3(a) allows horizontal shear transfer without inhibiting vertical movement. Fig. 3(d) shows a typical base detail.
- BRBs increase the ductility, strength and stiffness of the RWMF. They can be highly instrumental in implementing drift control, damage reduction and CP strategies. The challenge therefore, is to select the brace force $T_{B,r,i}$, at r^{th} stage loading, for i^{th} level sub frame, in such a way as to reduce the effects of the external moments including the *P*-delta and out of straightness ϕ' effects, Fig. 1(l), to more

manageable levels. This is achieved by defining an equivalent moment of resistance $M_{B.r}$ and equivalent rotational stiffness $K_{B.r}$ for the braced frame of Fig. 1 (b).

The conceptual development presented herein is based on the assumption that the MF can be modeled as imaginary subframes stacked on top of each other, Fig.1 (e). The RWMF is subjected to two groups of external moments, opposed by as many internal resisting moments as there are groups of resisting elements. The external overturning moment $M_{0.r}$ is caused by the lateral forces $F_{r,i}$ and the *P*-delta moment, $M_{P\Delta.r}$. The internal global moments; $M_{F.r}, M_{D.r}, M_{B.r}$ and $M_{C.r}$ are due to the resistance of the members of the MF, LBs, BRBs and the RRW respectively at r^{th} stage loading. The load-displacement relationship of each group of components of each sub frame *i*, such as $M_{F.r,i}$, is derived separately. All subframe moments are then superimposed to establish the global force displacement relationship of the system. The purpose of the current section is to develop a closed form formula for the response of the imaginary subframe throughout the loading history of the RWMF, starting from zero to MF failure, from MF failure to LB and BRB incapacitation and eventually the collapse of the structure. This could in turn be used to CP, life safety, immediate occupancy, etc. to Maximum Considered Earthquake ground motion intensity and other stipulated criteria. The following strategies have been implemented to reduce the task of complicated analysis to manageable static solutions, that;

- Instead of modeling the axial restraining effects of the LBs, BRBs and the RRW tendons, equivalent rotational schemes have been utilized to capture the restoring effects of these devices,
- The additional stiffness of a horizontal subframe containing a BRB, can be expressed as that of an equivalent pin-jointed subframe with modified properties, Fig. 5, and that,
- The redistribution of moments through formation of plastic hinges at beam ends, Fig. 4(b), due to sway type failure, forces the points of inflexion towards mid spans.

Since $\phi_{r,i} = \phi_r$ and imperfection ϕ', Fig.1(*l*), are the same for all sub frames *i* at r^{th} stage loading, then the drift equation of any subframe, as in Fig.1(e) in terms of story level racking $M_{0,r,i} = V_{r,i}h_i$ *P*-delta moments, $M_{P\Delta,r,i} = (\phi_r + \phi')h_i \sum_i^m \sum_{j=0}^n P_{i,j}$ and sub frame stiffness $K_{r,i}$ can be expressed, as;

$$\phi_{r,i} = \frac{(V_{r,i}h_i + M_{P\Delta,r,i})}{12E}\left[\frac{1}{\sum_{j=0}^n \bar{\delta}_{i,j} k_{col.i,j}} + \frac{1}{2\sum_{i=1}^n \delta_{i,j} k_{beam,i,j}}\right] = \frac{(M_{0,r,i} + M_{P\Delta,r,i})}{K_{r,i}h_i^2} \tag{1}$$

E is the modulus of elasticity, $k_{col.i,j} = J_{i,j} / h_i$ and $k_{beam,i,j} = I_{i,j} / L_j$ are relative stiffness's. $P_{i,j}$ and $P_i = \sum_i^m \sum_{j=0}^n P_{i,j}$ are nodal and total accumulative gravity loads acting on level *i* respectively. The Kronecker's deltas $\delta_{i,j}^P$ and $\bar{\delta}_{i,j}$ have been introduced to help track the response of the structure as a continuum, they refer to the effects of formation or lack of formation of plastic hinges at the ends of beams *i, j*. For instance, $\delta_{m,j}^P = 1$ if $M_{i,j} < M_{i,j}^P$ and $\delta_{i,j}^P = 0$ if $M_{i,j} = M_{i,j}^P$. $\delta_{i,j}^P = 0$, also implies structural damage or loss of stiffness with respect to member *i,j*. $\bar{\delta}_{i,j}$ has been introduced to include the contribution or lack thereof column stiffness to overall stiffness $K_{r,i}$ due to the formation of plastic hinges at the ends of the adjoining beams. $\bar{\delta}_{i,j} = 0$ if $M_{i,j} = M_{i,j}^P$ and $M_{i,j-1} = M_{i,j-1}^P$, otherwise $\bar{\delta}_{i,j} = 1$. M^P is the plastic moment of resistance. Next since the sum of story level moments; $(V_{r,i}h_i + M_{P\Delta,r,i})$ is equal to the total external overturning moment $(M_{0,r} + M_{P\Delta,r})$ it gives;

$$M_{0,r} + M_{P\Delta,r} = \sum_{i=1}^m (V_{r,i}h_i + M_{P\Delta.r,i}) = \sum_{i=1}^m \phi_{r,i} K_{r,i} h_i^2 \qquad \text{or} \quad \phi_r = \frac{M_{0,r} + M_{P\Delta,r}}{\sum_{i=1}^m K_{r,i} h_i^2} \tag{2}$$

The denominator of Eq. (2) represents the rotational stiffness of the un-supplemented RWMF under lateral and *P*-delta effects. It represents a closed form solution that can estimate lateral displacements

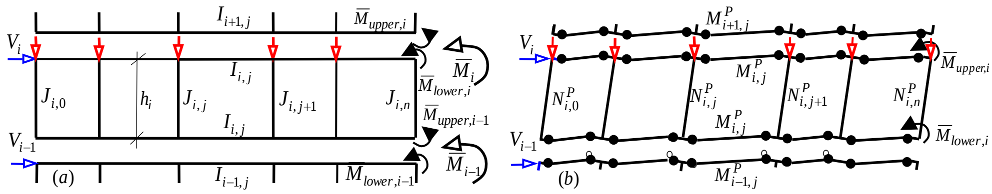

Figure 4. (a) Subframe under racking shear and LB moments, (b) Subframe plastic failure mechanism.

and member forces of RWMFs throughout the entire linear and nonlinear static ranges of loading. In Eq. (2) shear, panel zone, hinge offset, axial load and other secondary effects have been discarded in favor of simplicity. Eq. (2) is highly versatile in that it contains all plausible performance levels that affect structural response, safety and property protection.

2.1 Development of sub frame and LB load-displacement relationship

Since any two vertically stacked subframes share the same LB, it would be rational to divide the gap opening moment $\overline{M}_i = T_{L,i}d_i/2$ in proportion to their stiffness's, i.e., $\overline{M}_{upper,i} = I_{i+1}\overline{M}_i/(I_i + I_{i+1})$ and $\overline{M}_{lower,i} = I_i\overline{M}_i/(I_i + I_{i+1})$, where $T_{L.r,i} = T_{L.r}$ is the LB tensile force, Figs. 2(a) and (b). The magnitude of the gap rotation $\overline{\phi}$ can be expressed as a function of the LB length l and the adjoining wall and column offset distances D_{lft} and D_{rt}, respectively, Fig. 2(a), i.e.

$$\overline{\phi} = \left[\frac{D_{lft} + D_{rt} + 2l}{2l}\right]\phi = \alpha\phi \tag{3}$$

The relationship between the wall side gap opening and the corresponding tendon extension at any loading stage r may be expressed as;

$$\overline{\phi}_{r,i} = \alpha\phi_{r,i} = \frac{2T_{L.r,i}L_L}{dA_LE_L} = \frac{4T_{L.r,i}dL_{Lb}}{2d^2A_LE_L} = \frac{M_{D.r,i}}{K_D} \quad \text{and} \quad K_D = \frac{d^2A_LE_L}{4L_L} \tag{4}$$

Let E, A and L represent modulus of elasticity, cross-sectional area and length respectively. Suffixes L, B and W refer to link beams, braces and wall tendons respectively. The frame side column is not rigid. The drift reduction on a subframe due to opposing moments $\overline{M}$, Fig. 4(a) can be computed as;

$$\phi_{r,i} = \frac{(\overline{M}_{r,lower,i} + \overline{M}_{r,upper.i-1})}{24E}\left[\frac{1}{\sum_{j=1}^{n}\delta_{i,j}k_{beam.i,j}}\right] \tag{5}$$

However, for $I_i = I$ and $K_{D,i} = K_D$, $\overline{M}_{upper,i-1} = \overline{M}_{lower,i} = \overline{M}_i/2 = \overline{M} = T_f d/4$. Eq. (5) reduces to;

$$\varphi_{r,i} = \frac{\overline{M}_{r,i}}{12E}\left[\frac{1}{\sum_{j=1}^{n}\delta_{i,j}k_{beami,j}}\right] = \frac{\overline{M}_{r,i}}{\overline{K}_{r,i}} = \frac{(\alpha K_D\phi_{r,i})}{\overline{K}_{r,i}} = \overline{K}_{D.r,i}\phi_{r,i} \tag{6}$$

If there is m-s number of active LBs above level **s**, where, $0 \geq s \geq m$, then the total restoring moment of all activated sub frames, $M_{D,r}$ can be computed as;

$$M_{D,r} = \sum_{i=s}^{m}\overline{M}_{r,i} = \sum_{i=s}^{m}\phi_{r,i}\overline{K}_{r,i} \quad \text{or} \quad \phi_r = \frac{\sum_{i=s}^{m}\overline{M}_{r,i}}{\sum_{i=s}^{m}\overline{K}_{r,i}} = \frac{\alpha(m-s)K_D\varphi_{r,i}}{\sum_{i=s}^{m}\overline{K}_{r,i}} \tag{7}$$

The net effect of the overturning and opposing moments on the MF can be computed as;

$$\phi_r = \frac{(M_{r,0} + M_{P\Delta,r})}{K_{F,r}} - \varphi_r = \frac{(M_{r,0} + M_{P\Delta,r})}{K_{F,r}} - \overline{K}_{D,r}\phi_r \quad \text{or} \quad \phi_r = \frac{(M_{r,0} + M_{P\Delta,r})}{(1+\overline{K}_{D,r})K_{F.r}} \tag{8}$$

where, $\overline{K}_{D.r} = \alpha(m-s)K_D/\sum_{i=s}^{m}\overline{K}_{r,i}$ and $(1+\overline{K}_{D.r,i})K_{F.r}$ are the contributions of the frame side LBs and the equivalent stiffness of the subframe respectively. If all active LBs can develop their ultimate moments of resistance $M_{D,i}^{P} = \overline{M}_{upper,i}^{P} + \overline{M}_{lower,i+1}^{P}$, then the ultimate carrying capacity of the MF, including the LBs becomes;

$$(M_0^P + M_{P\Delta}^P) = 2\sum_{i=s}^{m} M_{D,i}^P + 2\sum_{j=1}^{n}\sum_{i=0}^{m} \overline{M}_{i,j}^P \tag{9}$$

As I_i tend toward zero, the rotational springs prevent subframe collapse, and Eq. (8) reduces to;

$$\phi_P = \frac{M_0^P + M_{P\Delta}^P}{\alpha(m-s)K_D} \tag{10}$$

2.2 Development of sub frame and BRB load-displacement relationship

Consider the displacements of the imaginary braced frame of Fig.1, composed of the end column at $j=n$ and the RRW as its vertical chords, and LBs and BRBs as its horizontal and diagonal elements respectively. The RRW imposes a straight drift profile on the MF and the braced frame. As a result, each subframe, such as that shown in Fig. 5(b), displaces an amount $\Delta_{r,i} = \phi_r h_i$, with respect to its lower chord. The challenge here is to relate the brace force $T_{B.r,i}$ to the drift ratio ϕ_r. This is achieved by assuming all members of the MF are axially rigid and constitute an unstable mechanism, Fig. 5(a). The axial deformation Δ_i of any such brace can be related to the uniform drift ratio, i.e.

$$\Delta_{r,i} = \frac{\alpha\phi_r h_i l}{\overline{L}_{B.i}} = \frac{T_{B.r,i}\overline{L}_B}{A_{B.i}E_B} \;,\quad T_{B.r,i} = \frac{\alpha\phi_r h_i l A_{B,i}E_B}{\overline{L}_{B.i}^2} \quad \text{or} \quad A_{B,i} = \frac{T_{B.r,i}\overline{L}_{B.i}^2}{\alpha\phi_r h_i l E_B} \tag{11}$$

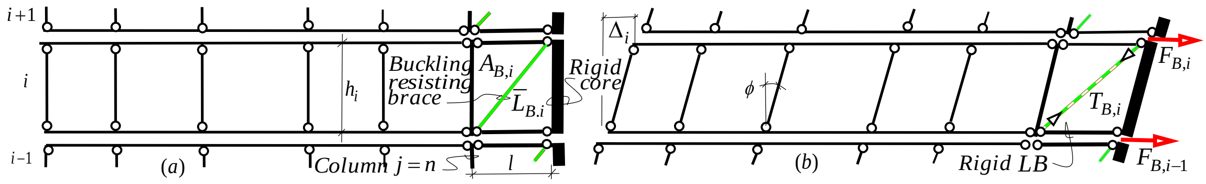

Figure 5. (a) Subframe ***i*** and BRB before rotation, (b) Subframe ***i*** and BRB after rotation

Let $F_{B.r,i}$ stand for the equivalent notional lateral load corresponding to BRB force $T_{B.r,i}$ of Fig.5 (b). Next, consider the compatible rigid body rotations, $\phi_{B.r}$ of all sub frames. If there is *m-u* number of BRBs above level $u, 0 \geq u \geq m$, then the corresponding virtual work equation can be written down as;

$$\sum_{i=u}^{m} F_{B.r,i}\varphi_r x_i = \varphi_r M_{B,r} = \sum_{i=u}^{m} T_{B.r,i}\Delta_{r,i} = \sum_{i=u}^{m}\left[\frac{\alpha^2\varphi_r{}^2 h_i^2 l^2 A_{B,i}E_B}{\overline{L}_{B.i}^3}\right] \tag{12}$$

$$\text{or } \varphi_{B,r} = \frac{M_{B,r}}{\alpha^2 l^2 E_B \sum_{i=u}^{m}(h_i^2 A_{B,i}/\overline{L}_{B.i}^3)} = \frac{M_{B,r}}{K_{B,r}} \tag{13}$$

This implies that the braced frame tends to oppose the external overturning moment by a notional global moment of resistance related to the axial resistance of the BRBs. Following Eq. (8), it gives;

$$\phi_r = \frac{(M_{0,r} + M_{P\Delta.r}) - M_{B,r}}{(1+\overline{K}_{D,r})K_{F,r}}, \qquad \text{or} \qquad \phi_r = \frac{(M_{0,r} + M_{P\Delta.r})}{K_{B,r} + (1+\overline{K}_{D,r})K_{F,r}} \tag{14}$$

However, it is expedient to deal with a single force $F_{B,m} = T_m l/\overline{L}_m$ as shown in Fig. 1(f) rather than the generalised distribution of forces $F_{B,i}$ of the same figure that result in a stepwise variation of shear forces along the frame. The brace force distribution due to the former strategy can be expressed as; $T_m = F_{B,m}\overline{L}_m / l,...$, $T_i = F_{B,m}\overline{L}_i / l,...$, and $T_1 = F_{B,m}\overline{L}_1 / l$. This allows all brace sectional areas $A_{B,i}$ to be related to any known value such as $A_{B,m}$,i.e., $A_{B,i} = (\bar{L}_i / \bar{L}_m)^3 (h_m / h_i) A_{B,m}$. Since all brace forces are functions of the same variable ϕ and that internal forces of all members are in static equilibrium, then the global moment due to brace resistance can be directly assessed as; $M_B = T_m l H / \bar{L}_m$. If M_B reaches its ultimate value, then the total carrying capacity of the system can be estimated as;

$$\sum_{i=1}^{m} F_{B,i}^{P} x_i = M_B^P = \sum_{i=1}^{m} T_{ult,i} \frac{\alpha h_i l}{\bar{L}_{B.i}} \tag{15}$$

If ϕ exceeds $\phi_{Rqd.}$, or $K_{F,r}$ is deemed inadequate, then Eq. (15) may be utilized to assess the additional stiffnesses of the BRBs required to satisfy the prescribed requirements.

$$K_{B.r} = \frac{(M_{0,r} + M_{P\Delta,r}) - \phi_r (1 + \bar{K}_{D.r}) K_{F,r}}{\phi_r} \tag{16}$$

2.3 Development of MF and RRW displacement relationship

The pair of parallel unbonded tendons and the pivot at the base constitutes a rotational spring of stiffness K_C, designed to remain elastic during and after an earthquake. The stress-strain relationship of the base spring at any loading stage *r*, can be expressed as a function of $\phi_r = M_{C,r} / K_{C,r}$, where $M_{C,r}$ represents the moment of resistance of the spring due to ϕ_r, i.e., $\phi_r d' = \varepsilon_{W.r} L_W$. Substitution of $\varepsilon_{W.r} = T_{W.r} / A_W E_W$ and $M_{C,r} = T_{W,r} d'$ in the strain equation gives $K_{C,r} = d'^2 A_W E_W / L_W$ Following Eq. (14), the contribution of K_C to the response of the RWMF can be examined as;

$$\phi_r = \frac{(M_{0,r} + M_{P\Delta.r}) - M_{C,r}}{K_{B.r} + (1 + \bar{K}_{D.r}) K_{F.r}} \text{ or } \phi_r = \frac{(M_{0,r} + M_{P\Delta.r})}{K_{C.r} + K_{B.r} + (1 + \bar{K}_{D.r}) K_{F.r}} = \frac{(M_{0,r} + M_{P\Delta.r})}{K_r^*} \tag{17}$$

Eq. (17) is the most generalized characteristic load-displacement equation of the RWMF, where K_r^* represents the global stiffness of the system at any loading stage *r*. K_r^* contains a continuum of ten distinct and several intermediate levels of response; $r = 0$, $r = E$, $r = Y$, $r = C$, $r = B_E$, $r = B_Y$, $r = L_E$, $r = L_Y$, $r = C_E$, $r = C_Y$ or $r = W$ Intermediate levels can be defined in terms of fractions of stages of *r*, e.g., *r*=0.6Yield or *r*=0.3 Device etc.

3. EFFECTS OF INITIAL IMPERFECTIONS AND *P*-DELTA MOMENTS

Initial imperfections occur due to a number of reasons including; construction inaccuracies, foundation failure, shrinkage, residual displacements etc. However, noting that $M_{P\Delta,r} = \sum_{i=1}^{m} \sum_{j=0}^{n} P_{i,j} (\phi_r + \phi') x_i = (\phi_r + \phi') P^* \bar{H}$, Eq. (17) can also be re-written as;

$$\phi_r = \frac{M_{0.r} + \bar{M}_{0.}}{f_{Cr,r} [K_{C.r} + K_{B.r} + (1 + \bar{K}_{D.r}) K_{F.r}]} = \frac{M_{0,r} + \bar{M}_0}{f_{CR.,r}^* K_r^*} \quad \text{and} \quad \bar{M}_0 = P^* \bar{H} \bar{\phi} \tag{18}$$

$f_{Cr.r}^* = [1 - P^* \bar{H} / K_r^*]$ is the global load reduction factor due to destabilizing effects of $P^* = \sum_{i=1}^{m} \sum_{j=0}^{n} P_{i,j}$ acting at the center of gravity of P^* at $\bar{H}$. Finally, if a state of damage tolerant design is specified, then Eq. (18) would have to be amended by replacing $(M_{0.r} + \bar{M}_0)$ and $(1 + \bar{K}_{D.r}) K_{F.r}$, with $(M_0^P + M_{P\Delta}^P)$ and $\alpha (m - s) K_D$ respectively.

4. NONLINEAR STATIC ANALYSES

RWMFs being SDOF systems are ideally suited for nonlinear static modeling, provides guidelines on the simplifying assumptions and limitations on nonlinear static seismic analysis procedures. The mathematical model described by Eqs. (17) and (18) contains the entire spectrum of nonlinear static responses and satisfies all conditions of the uniqueness theorem, and as such cannot be far from a minimum weight solution. If the plastic moments of resistance of the beams and supplementary devices are given by; $\bar{M}_{i,j}^{P}$, $M_{D,i}^{P}$, $M_{B,i}^{P}$ and M_{C}^{P} respectively, then;

$$(M_0^P + M_{P\Delta}^P) = M_C^P + 2\sum_{i=s}^{m} M_{D.i}^P + \sum_{i=u}^{m} M_{B,i}^P + 2\sum_{j=1}^{n}\sum_{i=0}^{m} \bar{M}_{i,j}^P \quad (19)$$

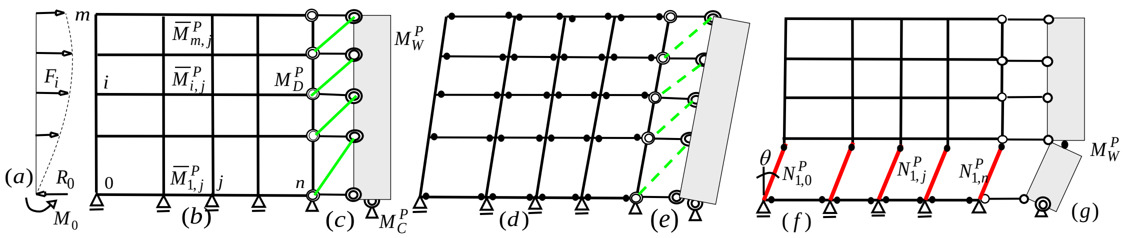

Figure 6. (b) RRMF, (c) RRW, (d) MF failure, (e) BRB failure, (f) Soft story failure, (g) Wall failure

Once again, if a state of damage tolerant design is specified, then the last term in Eq. (19) would have to be replaced with its elastic counterpart, $2\sum_{j=1}^{n}\sum_{i=0}^{m}\bar{M}_{i,j}$. Eq.(19) can also be used to establish the load factor needed to assure CP and SC, in which case it would be appropriate to assume; $M_C^P > 2\sum_{i=0}^{m} M_{D,i}^P > M_B^P > 2\sum_{j=1}^{n}\sum_{i=1}^{m}\bar{M}_{i,j}^P$. Well-proportioned MFs of RWMF are designed to fail in a sway mode as opposed to involving a beam mechanism. The small load theorem for MFs provides limiting magnitudes for gravity loads below which no beam type failure mechanism can take place.

RWMF with no supplementary devices, $M_C^P = M_D^P = M_B^P = 0$

LBs do not provide rotational stiffness and transmit only axial forces. The MF is designed to fail in a purely sway mode as in Fig. 6(d). The corresponding carrying capacity can be related to the sum of the ultimate resistances of the subframes as;

$$(M_0^P + M_{P\Delta}^P) = 2\sum_{j=1}^{n}\sum_{i=0}^{m}\bar{M}_{i,j}^P \quad (20)$$

Note that the RRW cannot improve the carrying capacity of MF. Substitution of $K_F = K_C = K_D = K_B = 0$, into Eq. (17) leads to the relevant drift ratio described by Eq.(10) above.

RWMF with no wall mounted supplementary devices, $M_D^P = M_B^P = 0$ **and** $M_C^P \neq 0$

In this case, the LBs transmit axial forces only, the MF fails in a sway mode, with the wall tendons either remaining elastic or yielding in tension. The corresponding collapse load can be estimated as;

$$(M_0^P + M_{P\Delta}^P) = M_C^P + 2\sum_{j=1}^{n}\sum_{i=0}^{m}\bar{M}_{i,j}^P \quad (21)$$

The corresponding drift ratio can now be estimated by inserting $K_F = K_D = K_B = 0$ in Eq. (17). In conclusion, a properly designed rocking wall can actually prevent plastic collapse of the entire system.

Fully supplemented RWMF with no wall tendons $M_C^P = 0$, $M_D^P \neq 0$ and $M_B^P \neq 0$

In this particular case the MF will also fail in a purely sway mode, with the LB tendons remaining elastic or yielding in tension. The corresponding collapse load can be computed as;

$$(M_0^P + M_{P\Delta}^P) = 2\sum_{i=s}^{m} M_{D,i}^P + 2\sum_{j=1}^{n}\sum_{i=0}^{m} \bar{M}_{i,j}^P + \sum_{i=u}^{m} M_B^P \tag{22}$$

Following the arguments leading to Eq. (17), the drift ratio can now be computed by replacing $K_i h_i^2(1+\bar{K}_{D,i})$ with $\alpha K_{D,i}$ and inserting $K_C = 0$ in Eq. (17). The stability of the MF suggests that a well-designed LBs and BRBs, can either on their own or in conjunction with a properly designed, pre-tensioned RRW help prevent total collapse and re-center the system after a seismic event.

5. DETERMINATION OF WALL STRENGTH

$K_D = K_B = K_C = 0$ -The purpose of this section is to establish the strength of the wall in such a way as to prevent soft story failure and to show that a well controlled design can meet both the target drift as well as the prescribed demand-capacity requirements. Since the RRW is a mechanism, it cannot enhance the carrying capacity of its companion frame at collapse, but its own capacity need not be less than the demand imposed upon it by the interactive forces Q_m and S_i shown in Figs. 1(g) and (h). The largest expenditure of energy is generally associated with first level soft story failure, as depicted in Figs. 6(f) and (g). If the plastic moments of resistance of the columns are deliberately selected as; $N_{i,j}^P = \lambda(M_{i,j}^P + M_{i,j-1}^P)$, where $\lambda > 1$ is the column over strength factor, then the virtual work equation for this failure mode can be expressed as, $M_0^P\theta + P^* h_1\theta = 2\sum_{j=1}^{n}\bar{M}_{1,j}^P\theta + \sum_{j=0}^{n} N_{1,j}^P\theta + M_w^P\theta$ which yields the wall strength as;

$$M_w^P > 2\sum_{j=1}^{n}\bar{M}_{1,j}^P + \sum_{j=0}^{n} N_{1,j}^P - (M_0^P + P^* h_1) \tag{23}$$

With M_0^P known, the value of M_w^P can be extracted from Eq. (23). The use of Eq. (23) is demonstrated in Appendix 1.

6. RWMF DESIGN STRATEGIES

A wide range of design strategies, depending on the nature of the interactive forces S_i can be envisaged. Forces S_i are needed to design the elements of the LBs and the RRW. The superposition of results of sections 3.1.1 through 3.1.4 leads to the expanded version of the characteristic equation of bending of subframe *i* at response stage *r*, i.e.,

$$(V_{r,i}h_i + M_{P\Delta.r,i}) = \phi_r[K_{C.r,i} + K_{B.r,i} + (1+\bar{K}_{D.r,i})K_{F.r,i}] = \phi_r K_{r,i}^* \tag{24}$$

Consider the combined effects of the external forces F_i and reactive forces Q_m and S_i of Figs.1 (g) and (h) on the subject MF, then for *i*=*m*, and $V_m = F_m + Q_m - S_m$, Eq. (24) gives;

$$V_{r,m} = F_{r,m} + Q_{r,m} - S_{r,m} = \phi_r[K_{r,m}^* / h_m - P_m] \tag{25}$$

Application of Eq. (25) for *i*=*m*-1 yields;

$$V_{r,m-1} = F_{r,m} + F_{r,m-1} + Q_{r,m} - S_{r,m} - S_{r,m-1} = \phi_r[K_{r,m-1}^* / h_{m-1} - P_{m-1}] \tag{26}$$

Subtracting (25) from (26) and rearranging gives;

$$V_{r.m-1} - V_{r,m} = F_{r,m-1} - S_{r,m-1} = \phi_r[(K_{r,m-1}^*/h_{m-1}) - (K_{r,m}^*/h_m) - (P_{m-1} - P_m)] \tag{27}$$

It follows therefore that with ϕ_r available from Eq. (17), $S_{i,r}$ can be computed as;

$$S_{r,i} = F_{r,i} - \phi_r[(K_{r,i}^*/h_i) - (K_{r,i+1}^*/h_{i+1}) - (P_i - P_{i+1})] \tag{28}$$

While Eq. (28) contains a large number of solutions, two extreme but important scenarios come to mind, $S_i = 0_i$ and $S_i = F_i$. The two limiting cases describe the use of RWMF combinations as, either counterproductive, or highly efficient. These limiting cases are known as MFs of Uniform Sections or Uniform Shear (MFUS) and MFs of Uniform Response (MFUR) respectively. The attributes of both cases are briefly discussed in sections 5.1 and 5.2 below.

Case 1, $S_{r,i} = 0$**, Attributes of MFUR-** The first case implies no wall-frame interaction, i.e., either $E_w I_w = 0$ or the free standing MF is an MFUR, Fig. A (a). In MFUR, groups of members such as beams and columns respond identically to external forces. Elements of the same group are designed to simultaneously undergo identical deformations and to develop equal stresses throughout the structure, Grigorian (2011). MFUR act as frameworks of equal strength and stiffness in which members of the same group share the same demand-capacity ratios regardless of their location within the system. Substituting $S_{r,i} = 0$ and $F_{r,i} = V_{r,i} - V_{r,i+1}$ in Eq. (28), gives;

$$F_{r,i} = \phi_r[(K^*_{r,i} / h_i) - (K^*_{r,i+1} / h_{i+1}) - P_i] \tag{29}$$

Since ϕ_r is constant for all *i*, then Eqs. (25) and (26) lead to the interpretation that;

$$\phi_r = \frac{V_{r,m}h_m}{K^*_{r,m} - P_m h_m} = \frac{V_{r,i}h_i}{K^*_{r,i} - P_i h_i} \tag{30}$$

In MFUR the demand-capacity ratios for groups of elements such as beams, columns, connections, etc., remain constant during all phases of loading, and as such;

$$M_i^P = \left(\frac{V_i}{V_m}\right)\left(\frac{h_i}{h_m}\right)\left(\frac{1 - P_m / K_m h_m}{1 - P_i / K_i h_i}\right) M_m^P \tag{31}$$

MFUR are optimized systems that are used to assess the efficiencies of identical MFs under similar loading. Since $\phi_i = \phi$ and the frame obeys the rules of proportionality, it can no longer benefit from the stiffness of the wall. The conclusion drawn here is that it would be unproductive to use RRWs in conjunction with MFUR. The attributes of a typical MFUR are briefly illustrated in Appendix 2.

Case 2 $S_i = F_i$**, Attributes of MFUS-** MFUS can also be categorized as MFUR except that members of the same group of elements possess the same section properties, regardless of their location within the MF. The use of RRWs in conjunction with MFUS can be highly effective in improving the lateral resistance of otherwise poorly performing MFUS. The second scenario, $S_i = F_i$ and absorbs **the** external load, and that the MF obeys the rules of Eq. (27), i.e.

$$V_{r,i} - V_{r,i+1} = \phi_r[(K^*_{r,i} / h_i) - (K^*_{r,i+1} / h_{i+1}) - (P_i - P_{i+1})] = 0 \tag{32}$$

Alternatively $\phi_{r.i} = \phi_r$ and $V_{r,i} = V_r$ are constant for the same *r* along the height of the structure, or

$$\phi_r = \frac{V_{r,m}h_m}{K^*_{r,m} - P_m h_m} = \frac{V_{r,i}h_i}{K^*_{r,i} - P_i h_i} \tag{33}$$

Since $S_i = F_i$ then the generalized rocking wall equilibrium equation may be rewritten as;

$$Q_{r,m} H + [K_{C.r} + (m-s)K_{D.r} - (M_{0,r} + M_{P\Delta.r}) = 0 \tag{34}$$

The free body diagrams of the subframes and the rocking wall of the subject RWMF are shown in Figs. A(c) through A(f). The resulting frame as depicted in Fig. A(c) is known as an MFUS. While the use of free standing MFUS may appear counterintuitive, their combination with properly designed RRWs can lead to the development of highly efficient RWMFs. An even more counterintuitive but highly efficient condition arises when $h_i = h.$ For equal or nearly equal story heights, $K_{u,i} = K_u$, i.e., $I_{i,j} = I,$ implying that all horizontal members can be the same. Similarly, since $J_{i,j} = J$, all columns can also be the same. Appendix 3 provides a comparison between the performances of an idealized MFUS and a seemingly inefficient MFUS as part of a simple RWMF without supplementary devices.

7. DETERMINATION OF WALL STIFFNESS

The nature of the interactive forces S_i and Q_m suggests that the wall tends to bend as an upright simply supported beam with a rigid body tilt ϕ . In conclusion that the stiffer the wall, the better the performance of the RWMF. The reactive forces reach their maxima, as the wall becomes stiffer. However if the rigidity of the wall, were to be large but finite and $h_i = h,$ then the following design data in the form of maximum wall drift or end slope $\psi_{\max}$ may be found useful for preliminary estimation of wall stiffnesses under commonly occurring distributions of lateral forces, e.g.;

Uniform load: $$\psi_{\max} = \frac{Fh^2 m(m-1)(m^2+m-2)}{24E_w I_w}, \quad I_{w,\min} = \frac{Fh^2(m-1)(m^2+m-2)}{24E_w \varepsilon\phi} \tag{35}$$

Triangular: $$\psi_{\max} = \frac{Fh^2(m-1)(2m-1)(2m^2+3m-4)}{180E_w I_w m}, \quad I_{w,\min} = \frac{Fh^2(m-1)(2m-1)(2m^2+3m-4)}{180E_w \varepsilon\phi m} \tag{36}$$

In practice the stiffness can be related to a fraction of the uniform drift say $5\%\phi$ or $\psi_{\max} = \varepsilon\phi.$

8. COLLAPSE PREVENTION AND SELF CENTERING

Most guidelines for the rehabilitation of existing buildings define specific performance levels for immediate occupancy, life safety, and CP, where CP is defined as “the post earthquake damage state in which the building is on the verge of partial or total collapse”. The current section focuses briefly on CP employing RWMF technologies for both new as-well-as existing structures. Seismic collapse is usually triggered by structural instability or the *P*-delta phenomenon, preceded by the formation of partial or complete ductile failure modes. Plastic failure modes such as those shown in Figs. 6(d) and 6(f) undergo large lateral displacements that lead to catastrophic collapse. While gravity forces, as active components of the *P*-delta effect, are constant quantities, lateral displacements can be controlled even reversed by means of RWMF capabilities suggested by Eqs. (17) or (18), provided that residual effects are small, the wall remains elastic and suppresses soft story failure. The proposed structural system contains three drift-restraining mechanisms, the post-tensioned RRW, the LBs and the BRBs. These devices can be utilized either on their own or in combination with each other. The formation of the plastic failure mechanism implies that all K_i are zero. Therefore, the global stiffness of the combined system reduces to; $K^* = K_C + K_B + 2\alpha\sum_{i=0}^{m} K_{D,i}$. In other words if complete collapse is to be prevented after formation of the preferred plastic mechanism, then the surviving LBs, BRBs and the vertical cable system should be strong enough to withstand the entire conditional demand. However, it would be safe to assume that for all practical purposes the PT wall alone is capable of withstanding the earthquake induced *P*-delta effects, in which case the pertinent global stiffness maybe estimated at $K^* = K_C.$ The PT tendons not only act as lateral stabilizers, but also add strength and stiffness to the frame and the wall. Their inherent elasticity helps re-center the structure after an earthquake. The rotational stiffness of the base level cable arrangement has been defined as; $K_{C,r} = d'^2 A_W E_W / L_W$. With P^* and $\phi_{collapse}$ known, the required parameters for CP can be computed as; $T_w > \Omega(M_0 + \overline{M}_0)/d' = \Omega(2M_0 + P^* \phi_{collapse} \overline{H})/2d'$ and

$$A_W E_W = T_w H / \phi_{collapse} d' \tag{37}$$

Following Eq. (37) the total horizontal tendon force composed of initial tendon force $T_{W,0}$ and that due to additional extensions can be shown to be equal to;

$$T_w = T_{W,0} + 2d' \left[\frac{(E_C A_C / H)(E_T A_T / L_T)}{(E_C A_C / H) + E_T A_T / L_T} \right] \phi \tag{38}$$

Subscripts C and T refer to concrete and tendon respectively. Here, the wall height, H and the cable length L_T are not necessarily the same. T_W should be sufficiently large to re-center the structure, otherwise residual deformations can significantly affect the SC capacity of the system.

9. CONCLUSIONS

A relatively new seismic structural system that combines BRBs, LBs and RRWs with GBRMFs has been introduced. In addition to BRBs, both vertical as well as horizontal gap opening devices have been provided to ensure CP and active RC. PT provides restoring forces at the ends of the LBs and the RRW that tend to prevent catastrophic collapse and force the frame and the wall to return to their pre-earthquake positions. Several theoretically exact formulae for the preliminary design of regular RWMFs have been presented. The proposed concepts lead to minimum weight solutions. A new gap opening LB that does not induce unwanted moments in the columns and the diaphragms has also been introduced. In the interim two new classes of moment frames, MFUR and MFUS have also been introduced. It has been argued that the use of RRWs in conjunction with MFUR is counterproductive. In contrast the MFUS-RRW combination can lead to highly efficient earthquake resisting buildings.

9. REFERENCES

Grigorian M, Tavousi S, 2017a. Innovations in rocking wall-frame systems-Theory and development, *Int. J. Adv. Struct. Eng*. 9:205-217. DOI 10.1007/s40091-017-0165-x.

Grigorian M, Grigorian C, 2017b. Sustainable Earthquake-Resisting System, *J. Struct. Div*. ASCE, DOI: 10.1061/(ASCE)ST.1943-541X.0001900.

APPENDIX 1 - Example 1, minimum wall strength

Let, $F_i = Fi/m$, $P_{i,j} = \phi' = 0$, $\overline{M}^P_{i,j} = \overline{M}^P$, $\overline{M}^P_{0,j} = \overline{M}^P_{m,j} = \overline{M}^P/2$, $N^P_{1,0} = N^P_{1,n} = \lambda \overline{M}^P/2$, $N^P_{i,j} = \lambda \overline{M}^P$ for all other j and $h_i = h$. **Solution:** It can be shown that $M_0 = (m+1)(2m+1)Fh/6$ and $2\sum_{j=1}^{n}\sum_{i=1}^{m} \overline{M}^P_{i,j} = 2mn\overline{M}^P$, i.e., $F = 12mn\overline{M}^P/(m+1)(2m+1)h$. Similarly, Eq. (23) reduces to $\frac{Fh(m+1)}{2} = \frac{n\overline{M}^P}{2} + n\lambda \overline{M}^P + M^P_w$. Equating the last two equations for F, it gives;

$$M^P_w > \left[\frac{6m - (1+\lambda)(2m+1)}{(2m+1)} \right] n\overline{M}^P \tag{A-1}$$

APPENDIX 2 - Example 2, a typical MFUR

Consider the performance of the MFUR of Fig. 7(b) subjected to forces Fi/m with the following member properties: $I_{m,j} = I_m = I$, $J_{m,j} = 2.4I$ except for $J_{m,0} = J_{m,n} = J = 1.2I$. $M^P_{m,j} = M^P$, $N^P_{m,j} > 2M^P$ and $N^P_{m,0} = N^P_{m,5} > M^P$ for all other j. Assume $P_{i,j} = 0$, $K_{D,i} = \overline{K}_{D,i} = K_B = K_C = 0$. Following Eqs.(33) and (34) the corresponding subframe

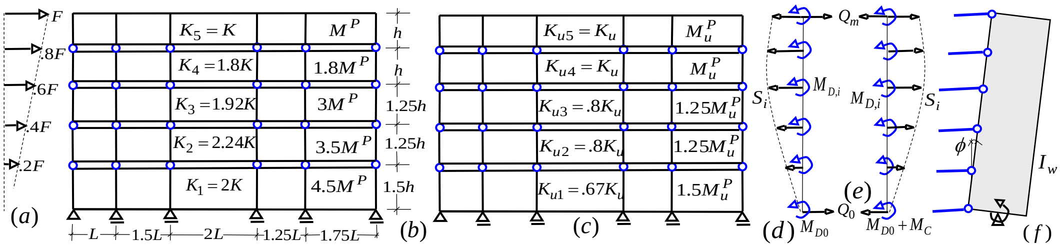

Figure 7. (a) Loading, (b) MFUR sub-frame stifnesses and plastic moments (c) MFUS sub-frame stifnesses and beam plastic moments (d) Interactive forces on MF (e) Interactive forces on RRW

stiffnesses K_i and moments M^P_i can be computed as shown in Fig. A(a). The MFUR failure load can be computed as $F^P = 20.00M^P / h$. The roof displacement and the uniform drift can now be estimated as; $\Delta_{MFUR} = \phi_{MFUR} 6h = 6F / K$ and $\phi_{MFUR} = F / Kh$ respectively. The complete elastoplastic solution to this frame can be found in. In additional this example can be used to assess the efficiency of the other extreme scenario where $S_i = F_i$.

APPENDIX 3-Example 3, a typical MFUS

The MFUS of Fig.7(c) is similar to the MFUR of Example 2. Following Eq.(32), the static equilibrium of the wall gives; $Q_{r,m} H = M_{r.0} = 13.8F_r h$ and $Q_{r,m} = 13.8F_r h / 6h = 2.3F_r$. Since the uniform drift rule, Eq.(33), can be simplified as $K_{r,i} = (h_m / h_i)K_{u,r,m} = K_u$, then the uniform drift and the maximum roof level displacement can be estimated as; $\phi_{MFUS} = Q / K_u h$ and $\Delta_{MFUS} = \phi_{MFUS} 6h = 6Q / K_u$ respectively. The MFUS plastic failure load can be shown to be equal to $F^P = 120.00M^P / 13.8h$. In order to compare the two systems, K_u should be selected in such a way that $\Delta_{MFUS} = \Delta_{MFUR}$. This gives $K_u = 2.3K$ for this particular example and leads to the general formula;

$$K_{u,m} = \frac{M_0}{F_m h_m} K_m \tag{A-2}$$

Next assuming that the unit weight of any sub-frame can be related to its plastic strength through a constant of proportionality γ, then the total weights of the MFUS and MFUR may be computed as;

$$G_{MFUS} = \gamma[2M^P_u + 2\times1.25M^P_u + 1.5M^P_u] = 6\gamma M^P_u = 0.69\gamma Fh \tag{A-3}$$